

---

# Transition Metals in Supramolecular Chemistry

*Perspectives in  
Supramolecular Chemistry  
Volume 5*

EDITED BY JEAN-PIERRE SAUVAGE

*Université Louis Pasteur, France*

JOHN WILEY & SONS

Chichester • New York • Weinheim • Brisbane • Singapore • Toronto



---

---

# **Transition Metals in Supramolecular Chemistry**

---

# Editorial Board

## Founding Editor

J.-M. Lehn, Collège de France, Chimie des Interactions Moléculaires, 11 Place Marcelin Berthelot, 75005 Paris, France

## Editors

J.-P. Behr, Faculté de Pharmacie, Université Louis Pasteur, Strasbourg, B.P. 24, F-67401, Illkirch, France

G.R. Desiraju, University of Hyderabad, School of Chemistry, Hyderabad 500134, India

A.D. Hamilton, Yale University, Department of Chemistry, New Haven, CT 06520, USA

T. Kunitake, Kyushu University, Faculty of Engineering, Hakozaki, Fukuoka 812, Japan

D.N. Reinhoudt, University of Twente, Faculty of Chemical Technology, P.O. Box 217, NL-7500 AE Enschede, The Netherlands

J.P.-Sauvage, Université Louis Pasteur, Institut le Bel, 4 Rue Blaise Pascal, F-67070 Strasbourg, France

---

# Transition Metals in Supramolecular Chemistry

*Perspectives in  
Supramolecular Chemistry  
Volume 5*

EDITED BY JEAN-PIERRE SAUVAGE

*Université Louis Pasteur, France*

JOHN WILEY & SONS

Chichester • New York • Weinheim • Brisbane • Singapore • Toronto

Copyright © 1999 John Wiley & Sons Ltd,  
Baffins Lane, Chichester,  
West Sussex PO19 1UD, England

National 01243 779777  
International (+44) 1243 779777

e-mail (for orders and customer service enquiries): [cs-books@wiley.co.uk](mailto:cs-books@wiley.co.uk)

Visit our Home Page on <http://www.wiley.co.uk>

or <http://www.wiley.com>

All Rights Reserved. No part of this publication may be reproduced, stored in a retrieval system, or transmitted, in any form or by any means, electronic, mechanical, photocopying, recording, scanning or otherwise, except under the terms of the Copyright Designs and Patents Act 1988 or under the terms of a licence issued by the Copyright Licensing Agency, 90 Tottenham Court Road, London W1P 9HE, UK, without the permission in writing of the publisher.

*Other Wiley Editorial Offices*

John Wiley & Sons, Inc., 605 Third Avenue,  
New York, NY 10158-0012, USA

WILEY-VCH Verlag GmbH, Pappelallee 3,  
D-69469 Weinheim, Germany

Jacaranda Wiley Ltd, 33 Park Road Milton,  
Queensland 4064, Australia

John Wiley Sons (Asia) Pte Ltd, Clementi Loop #02-01,  
Jim Xing Distripark, Singapore 129809

John Wiley & Sons (Canada) Ltd, 22 Worcester Road,  
Rexdale, Ontario M9W 1L1, Canada

***Library of Congress Cataloging-in-Publication Data***

Transition metals in supramolecular chemistry / edited by Jean-Pierre  
Sauvage.

p. cm. – (Perspectives in supramolecular chemistry ; v. 5)

Includes bibliographical references and index.

ISBN 0471-97620-2

1. Transition metal complexes. 2. Macromolecules. I. Sauvage,  
Jean-Pierre. II. Series.

QD474.T69 1999

546'.6–dc21

98-54677

CIP

***British Library Cataloguing in Publication Data***

A catalogue record for this book is available from the British Library

ISBN 0 471 97620 2

Typeset in 10/12pt Times by Techset Composition Ltd, Salisbury, Wiltshire

Printed and bound in Great Britain by Biddles Ltd, Guildford and King's Lynn

This book is printed on acid-free paper responsibly manufactured from sustainable forestry, in which at least two trees are planted for each one used for paper production.

---

# Contents

<b>Contributors</b>	vii
<b>Preface</b>	ix
<b>1 Ligand and Metal Control of Self-Assembly in Supramolecular Chemistry</b> Rolf W. Saalfrank and Bernhard Demleitner	1
<b>2 Bistability in Iron (II) Spin-Crossover Systems: A Supramolecular Function</b> José Antonio Real	53
<b>3 Fluorescent Sensors for and with Transition Metals</b> Luigi Fabbrizzi, Maurizio Licchelli, Piersandro Pallavicini, Luisa Parodi and Angelo Taglietti	93
<b>4 The Chirality of Polynuclear Transition Metal Complexes</b> Christophe Provent and Alan F. Williams	135
<b>5 Design and Serendipity in the Synthesis of Polymetallic Complexes of the 3d-Metals</b> Richard E. P. Winpenny	193
<b>6 Rotaxanes: From Random to Transition Metal-Templated Threading of Rings at the Molecular Level</b> Jean-Claude Chambron	225

<b>7 Metallomesogens—Supramolecular Organization of Metal Complexes in Fluid Phases</b>	
Simon Collinson and Duncan W. Bruce	285
<b>8 Self-Assembly of Interlocked Structures with Cucurbituril, Metal Ions and Metal Complexes</b>	
Kimoon Kim	371
<b>Cumulative Author Index</b>	403
<b>Cumulative Title Index</b>	407
<b>Index</b>	409



---

# Contributors

**Duncan W. Bruce**, School of Chemistry, University of Exeter, Stocker Road, Exeter, EX4 4QD, UK

**Jean-Claude Chambron**, Faculté de Chimie, Université Louis Pasteur, 67000 Strasbourg, France

**Simon Collinson**, School of Chemistry, University of Exeter, Stocker Road, Exeter, EX4 4QD, UK

**Bernhard Demleitner**, Institut für Organische Chemie der Universität Erlangen-Nürnberg, Henkestrasse 42, D-91054 Erlangen, Germany

**Luigi Fabbrizzi**, Dip. Chimica Generale, Università di Pavia, Via Taramelli 12, I-27100 Pavia, Italy

**Maurizio Licchelli**, Dip. Chimica Generale, Università di Pavia, Via Taramelli 12, I-27100 Pavia, Italy

**Kimoon Kim**, National Creative Research Initiative, Center for Smart Supramolecules and Department of Chemistry, Pohang University of Science and Technology, San 31, Hyojadong, Pohang 790-784, South Korea

**Piersandro Pallavicini**, Dip. Chimica Generale, Università di Pavia, Via Taramelli 12, I-27100 Pavia, Italy

**Luisa Parodi**, Dip. Chimica Generale, Università di Pavia, Via Taramelli 12, I-27100 Pavia, Italy

**Christophe Provent**, Département de Chimie Minérale, Analytique et Appliquée, Université de Genève, 30 quai Ernest Ansermet, CH 1211 Geneva 4, Switzerland

**José Antonio Real**, Departament de Química Inorgànica, Facultat de Química, Universitat de València, 46100 Burjassot, Spain

**Rolf W. Saalfrank**, Institut für Organische Chemie der Universität Erlangen-Nürnberg, Henkestrasse 42, D-91054 Erlangen, Germany

**Angelo Taglietti**, L Dip. Chimica Generale, Università di Pavia, Via Taramelli 12, I-27100 Pavia, Italy

**Alan F. Williams**, Département de Chimie Minérale, Analytique et Appliquée, Université de Genève, 30 quai Ernest Ansermet, CH 1211 Geneva 4, Switzerland

**Richard E. P. Winpenny**, Department of Chemistry, University of Edinburgh, West Mains Road, Edinburgh, EH9 3JJ, Scotland

---

# Preface

The pioneering work of Pedersen, Lehn and Cram on various cyclic structures acting as hosts, and their interactions with cationic species, is considered as the start of modern supramolecular chemistry—the chemistry of weak forces and noncovalent interactions. Clearly, 30 years ago transition metals and their complexes were not regarded as important components in such structures, and the fields of ‘host–guest’ recognition and coordination chemistry were very distinct with almost nothing to share. Things have dramatically changed! It suffices to wander through the eight following contributions to realize that transition metal complexes are nowadays used almost routinely to build large multicomponent architectures. These often display new and exciting properties on the way to molecular devices for specific functions.

Transition metals are utilized to construct fascinating structures such as ‘rotaxanes’ (a rotaxane is a ring threaded by an open-chain fragment bearing two bulky groups at its ends so as to prevent dethreading), or beautiful and novel multicomponent assemblies such as helices, grids and related high-nuclearity complexes. Another very active field of research, related to supramolecular sciences, is concerned with liquid crystals incorporating more and more sophisticated transition metal complexes and thus displaying increasingly well-defined and specific properties related to both their mesogen nature and the presence of transition metal centres.

Molecular magnetism constitutes another promising facet of modern coordination chemistry and the field has produced in recent years both magnificent solid-state structures and properties. The use of transition metal binding sites associated with various luminophores, for instance has also led to the development of promising molecular switches.

If the present volume covers a relatively broad field of coordination and supramolecular chemistry, I am conscious that other important related areas of research are not represented, in particular those related to biology. Nevertheless, this book gives an excellent and contemporary view of the ‘abiotic’ side, and we hope that it will contribute to stimulate ideas and interactions between researchers from various disciplines.

Jean-Pierre Sauvage  
*Strasbourg, May 27, 1998*



---

# Chapter 1

---

## Ligand and Metal Control of Self-Assembly in Supramolecular Chemistry

*ROLF W. SAALFRANK AND BERNHARD DEMLEITNER*

*University Erlangen-Nürnberg, Germany*

### 1 INTRODUCTION

Self-assembly [1–16] is ubiquitous in nature, where the process is used to create complex functional biological structures with precision. Biologically self-assembled structures are built up by a modular approach from simple, ordinary subunits, thus minimizing the amount of information required for a specific ensemble. Among the most notable biologically self-assembled structures is the *tobacco mosaic virus* (TMV) [17]. However, chemistry is not limited to systems similar to those found in nature; chemists are free to create unknown unnatural species and to invent novel processes. Driven by the quest for new host molecules, self-assembly has been recognized as a powerful methodology for the construction of supramolecular systems. The conceptual basis underlying self-assembled transition metal complexes makes structures generally analogous to the well-established organic-based molecular host–guest systems accessible. This analogy has proven highly successful for the controlled self-assembly of numerous clusters with predesigned molecular architectures. While much of the present work in supramolecular chemistry remains focused on the development of organic molecular recognition agents, there is an increasing interest in hosts that contain transition metals. Consequently, the predictable nature of coordination chemistry has been used successfully to generate the metallatopomers **4–6** of the coronates **1**, {2}-cryptates **2**, and {3}-cryptates **3**

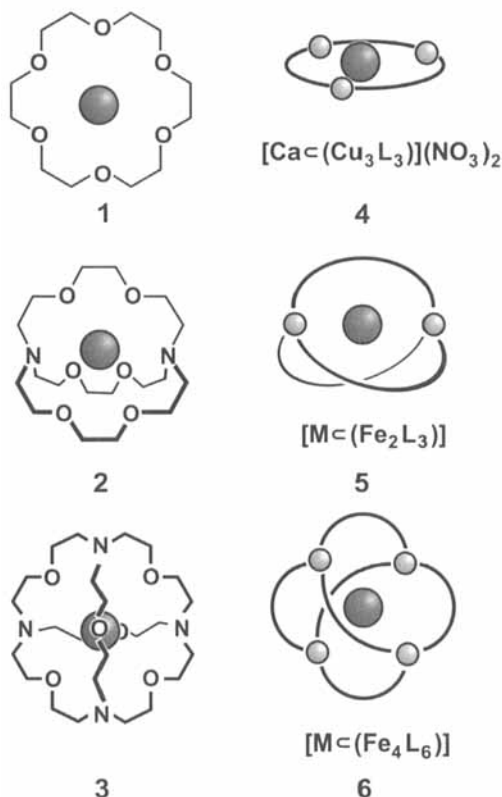


**Figure 1** Pictorial representation: metallatopomers 4–6 of coronates 1, {2}-cryptates 2, and {3}-cryptates 3.

efficiently by simply mixing the component ligands and metal ions in solution (Figure 1) [18,19].

These compounds enjoy a number of advantages over their organic counterparts, in particular, one-pot reactions, high yields, spectroscopic, electronic, and magnetic properties, which are inaccessible with organic species [20,21]. Furthermore, the use of transition metal coordination has been explored by Lehn and co-workers and many others. The new strategy was successfully used for the construction of molecular racks [1,22], ladders [1,11,23], grids [1,11,24,25], squares [7,26,27], cylinders [11,28], molecular boxes [29], catenanes [13,15,30], rotaxanes [31], knots [16,30,32], dendrimers [11,33], double, triple [12,13], and circular [34,35] helicites. Self-assembly of Werner-type complexes features the participation of weak, reversible, non-covalent bonding interactions, which facilitates error checking and self-correction. Over the years, the number of laboratories around the world, attracted by the interdisciplinary character of supramolecular chemistry, has increased consider-

ably. We do not attempt to cover the literature exhaustively, but more recent notable advances in this area have been given prominence here and are detailed below.

## 2 METALLACORONATES, CIRCULAR HELICATES, {2}-METALLACRYPTATES AND {3}-METALLACRYPTATES

### 2.1 Metallacoronands and Metallacoronates

Pecoraro *et al.* demonstrate [20] in an excellent comprehensive review article that cyclic structures generally analogous to classical organocrown ethers are accessible by simply substituting an ethane bridge with a transition metal ion. The metallacrown analogy has proven highly successful for the controlled preparation of homonuclear, heteronuclear, and mixed-valent assemblies of moderate nuclearity (3–12 metal atoms) with predesigned molecular architectures. Real metallacrown analogy [36] is nicely illustrated (Figure 2) by the trinuclear vanadium complex **7** [37,38], prepared from  $VCl_3$  with salicylhydroxamic acid and three equivalents of sodium methoxide in methanol. A series of related inorganic metallacrown copper(II) complexes have also been prepared and characterized by X-ray diffraction [39]. The tetranuclear copper(II) complex **8** [38,40], prepared with  $\beta$ -alanine-hydroxamic acid, displays an almost planar conformation of the macrocycle. Schematic diagrams of [9]crown-3 (9-C-3) **9** and [12]crown-4 (12-C-4) **10** are compared with the analogous cores of the metallacrowns [9]metallacrown-3 (9-MC-3) **7** and [12]metallacrown-4 (12-MC-4) **8**.

Salicylhydroxamic acid ( $H_3shi$ ), which contains both hydroximate and phenolate donors, and many hydroximate-based ligands form tri- and tetranuclear metallacrowns with moderate-to-high valent metal ions [e.g.  $Fe^{II}$ ,  $Mn^{III}$ ,  $Ga^{III}$ ] [20,21,39]. The  $shi^{3-}$  ligand combines a five- and a six-membered chelate ring and the next ligand is required to bind to this building block at a  $90^\circ$  angle (Figure 3). With rare exceptions, the molecules so far prepared can be realized in a one-step procedure with yields of crystalline product between 50 and 95%. The schematic diagrams of (9-MC-3) **7**, (12-MC-4) **11** and (15-MC-5) **12** demonstrate (Figures 2 and 3), that stable metallacrowns are not limited to a (9-MC-3) or (12-MC-4) motif. A logical concept for the predesigned synthesis of a planar (15-MC-5) structure is to alter the angle to  $108^\circ$  using picoline hydroxamic acid, which forms two five-membered chelate rings as shown for **12**.

#### 2.1.1 Trinuclear metallacoronands and metallacoronates

Crown ethers selectively complex alkaline ions [6,41], and the complexation of different sized cations leads to coronates [5,42] of various structures. The structural analogy between crown ethers and their topologically equivalent metallacrown ethers

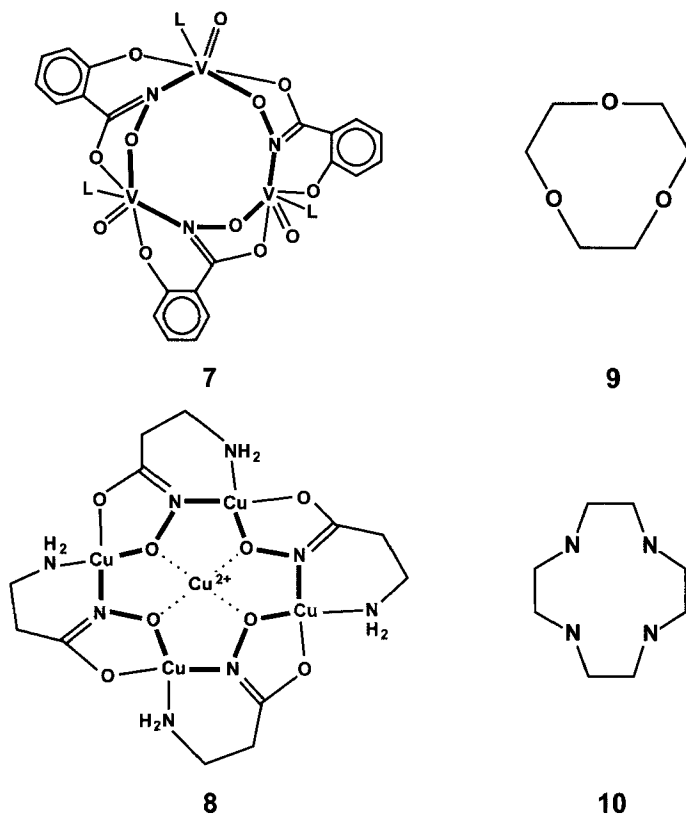


**Figure 2** Schematic diagrams of (9-C-3) **9** and (12-C-4) **10** compared with (9-MC-3) **7** and (12-MC-4) **8**.

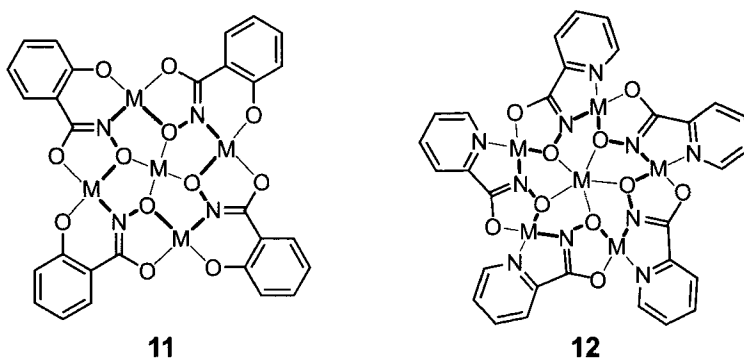
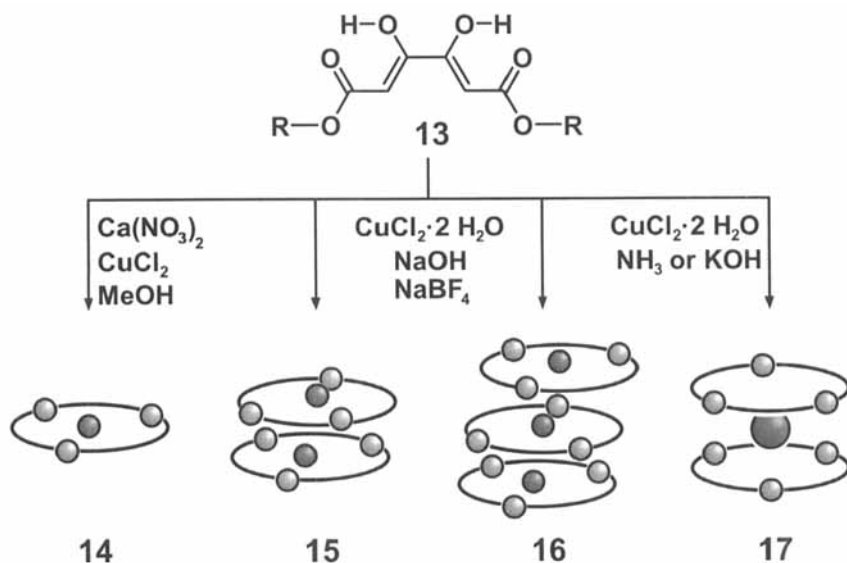


**Figure 3** Schematic diagrams of (12-MC-4) **11** and (15-MC-5) **12**.



(MC) [2,43–45] should lead to novel supramolecular architectures of well-defined host–guest compounds. Since the ionic radii of alkaline and alkaline earth metal cations differ significantly in size, whereas the diameter of a given metallacrown essentially does not change, the inclusion of small cations such as  $\text{Na}^+$  or  $\text{Ca}^{2+}$  should yield a metallacoronate [19,45–47] with 1 : 1 stoichiometry ( $\text{M}^+ : \text{MC} = 1 : 1$ ). On the contrary, encapsulation of the larger  $\text{K}^+$  or  $\text{NH}_4^+$  ions should lead to the formation of metallacrown ether sandwich complexes ( $\text{M}^+ : \text{MC} = 1 : 2$ ). Reaction of diethyl ketipinate  $\text{H}_2\text{L}$  **13** with copper(II) acetate in the presence of calcium nitrate affords green microcrystals **14** after crystallization from tetrahydrofuran/diethyl ether (Scheme 1).

According to the X-ray crystallographic analysis, metallacoronate **14** is a neutral trinuclear metal cluster of the general composition  $[\text{Ca} \subset (\text{Cu}_3\text{L}_3) \cdot (\text{NO}_3)_2] \cdot \text{THF} \cdot \text{H}_2\text{O}$ . The copper atoms are linked across the triangular corners by bis(bidentate) diethyl ketipinate dianions  $\text{L}^{2-}$ . Thereby each copper(II) ion is primarily coordinated in a square-planar fashion to four oxygen atoms. Additional coordination of water, tetrahydrofuran and nitrate, respectively, leads to a square-pyramidal environment of each copper(II) center by O donors. In the core of the resulting [15]metallacrown-6, a calcium ion is encapsulated, and for charge compensation, two nitrate ions are coordinated axially to calcium (Figure 4). Formal replacement of the three copper(II) centers in the calcium free [15]metallacrown-6 system of **14** by ethane bridges leads to the topologically equivalent [18]crown-6.



**Scheme 1** Formation of metallacoronate **14**, double-decker **15**, triple-decker **16**, and sandwich **17**.

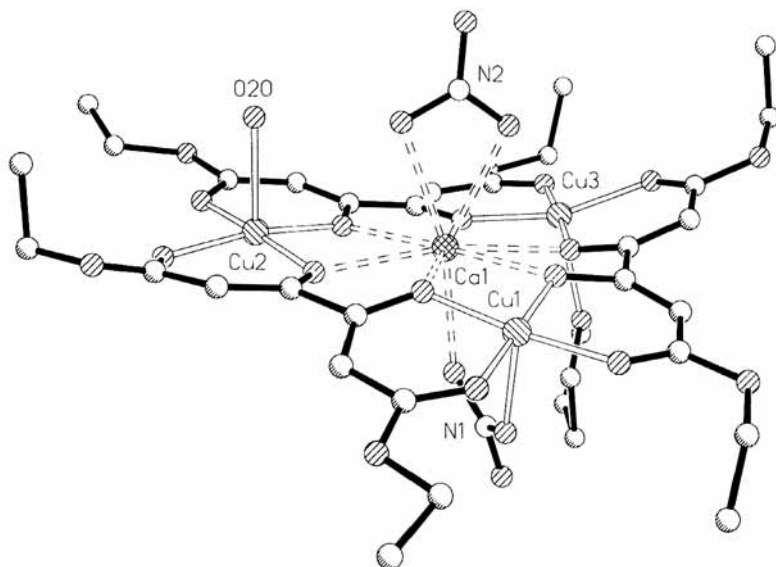


**Figure 4** X-ray crystallographic structure of trinuclear metallacoronate **14**.

Double deprotonation of diethyl ketipinate  $H_2L$  **13** by sodium hydroxide and reaction of the formed dianion with a methanolic solution of  $NaBF_4$  and copper(II) chloride dihydrate yields a mixture of two different crystalline metallacoronates **15** and **16** (Scheme 1), whose molecular structures were determined by X-ray crystallographic analyses. The metallacoronate **15** is a dimer of two  $[Na \subset (Cu_3L_3)BF_4]$  building blocks. The monomer is composed of a  $[Cu_3L_3]$  metallacrown with a sodium ion located in the core which is  $\eta^6$ -coordinated to all oxygen atoms in the inner ring. The counterion of the  $[Na \subset (Cu_3L_3)]^+$  cation is a  $BF_4^-$  ion. The eightfold donor solvation, the  $Na^+$  ions are striving for, leads to dimerization. The linkage of the monomers to give double-decker  $\{[Na \subset (Cu_3L_3)BF_4] \cdot THF \cdot H_2O\}_2$  **15** is accomplished via  $\eta^1$ -coordination of the two  $Na^+$  ions to one ring oxygen of each neighboring coronate. This leads to a minor mutual deformation of the monomeric building blocks (Figure 5).

However, similar suitable coordination around copper(II) and sodium is also achieved by the formation of triple-decker metallacoronate  $[Na \subset (Cu_3L_3)BF_4]_3 \cdot 2THF$  **16** (Figure 6; 3D-1). In order to accomplish eightfold coordination for the sodium ions, aggregation of the  $[Na \subset (Cu_3L_3)]^+$  monomers furnishes double- and triple-decker metallacoronates **15** and **16**. The features of stacking are governed by the coordination of water molecules. The coordination of water leads to the formation of dimeric complex **15**. In **15** both sites of the stack are totally coordinatively blocked by solvent molecules or tetrafluoroborate counterions. However, without coordination of water, the most suitable ligation around copper(II) and sodium is achieved by the formation of triple-decker metallacoronate **16**. A



common feature of **15** and **16** is their neutral, 15-membered building block. Formal replacement of the three copper(II) centers in the [15]metallacrown-6 fragments of **15** or **16** by ethane bridges leads to the topologically equivalent crown ether [18]crown-6.

Whereas, encapsulation of the small cations  $\text{Na}^+$  and  $\text{Ca}^{2+}$  leads to metallacoronates of 1:1 stoichiometry, double deprotonation of ketipinate  $\text{H}_2\text{L}$  **13** with potassium hydroxide and reaction with copper(II) chloride dihydrate affords metallacrown ether sandwich complex **17** with 2:1 stoichiometry (Scheme 1). The X-ray crystallographic analysis reveals that  $[\text{K} \subset (\text{Cu}_3\text{L}_3)_2\text{OMe}] \cdot 6\text{HOME}$  **17** is constructed of two neutral [15]metallacrown-6 building blocks which are turned relative to each other by  $60^\circ$ . The sandwich-like linkage results via a crystallographically disordered potassium ion in the center between the two metallacrowns. The counterion of the cation  $[\text{K} \subset (\text{Cu}_3\text{L}_3)_2] \cdot 6\text{HOME}^+$  of **17** is a methoxide ion, which is bound to the potassium ion. Coordinative saturation of the six copper centers results from methanol molecules. Thus, each  $\text{Cu}^{2+}$  ion is surrounded by O donors (Figure 7; 3D-2) in a tetragonal pyramidal geometry.

### 2.1.2 Hexa-, octa-, and decanuclear metallacoronands and metallacoronates

For a better understanding of electron transfer processes and of magnetic properties of polynuclear iron [48,49], manganese [50], and nickel complexes [51], further studies on compounds of this type are necessary. The same is true for metallacrown ethers with enclosed cations [38,43,44,51–53]. With respect to potential applications, iron(III) compounds certainly play a central role. Polyiron-oxo species are present in aqueous solution, but the growth of polyiron complexes cannot be controlled, and in the absence of additional ligands beyond oxo, hydroxo and aquo ligands, the final product of hydrolysis in water is ferrihydrite [53]. The situation is different in the presence of additional ligands. In fact, methanolysis of simple iron(III) salts in the presence of 1,3-diketonates has proved to be an excellent route to  $\text{Fe}_2$ ,  $\text{Fe}_3$ ,  $\text{Fe}_4$ ,  $\text{Fe}_6$ , and  $\text{Fe}_{10}$  clusters [54].

Several different types of  $\text{Fe}_6$  clusters have been reported, which were classified as planar, twisted boat, chair, parallel triangles, octahedral and fused clusters [55]. The  $[\text{Fe}_6(\mu_2\text{-OME})_{12}(\text{dbm})_6]$  ring, where Hdbm is dibenzoylmethane, is a neutral species, but in the solid state it crystallizes with NaCl to give **18** (Figure 8). In fact, the sodium ion is trapped in the center of the iron ring, which acts like a crown ether complexing the alkaline earth ion [53].

Recently, reaction of triethanolamine with sodium hydride and addition of iron(III) chloride in THF (Scheme 2) afforded yellow crystals of **19**, in which the iron-to-ligand ratio was 1:1 and the ratio of iron to sodium chloride was 6:1.

For the unequivocal characterization of the molecular structure of **19**, an X-ray crystallographic structure analysis was carried out [46]. According to this analysis, **19** is present in the crystal as a cyclic iron(III) complex with a [12]metallacrown-6

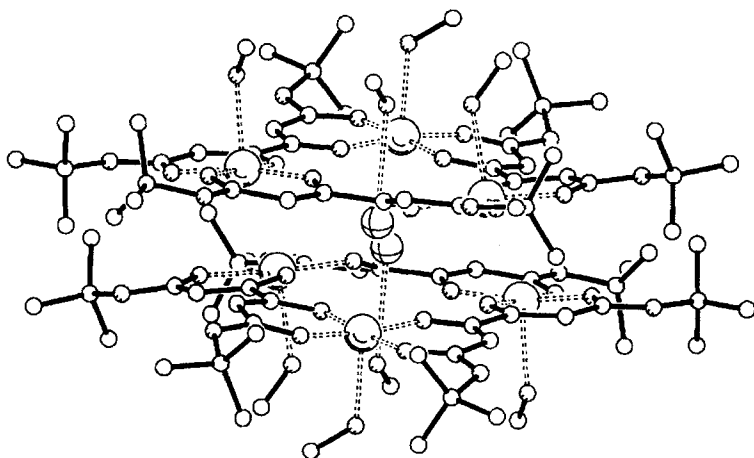


**Figure 7** X-ray crystallographic structure of sandwich  $[K C (Cu_3L_3)_2OMe] \cdot 6HOMe$  **17**, with  $K^+$  and  $MeO^-$  disordered.

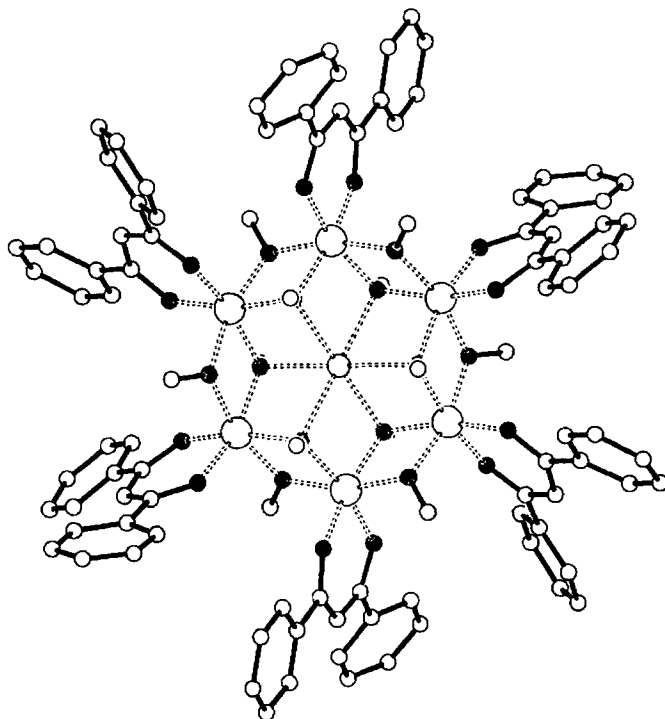
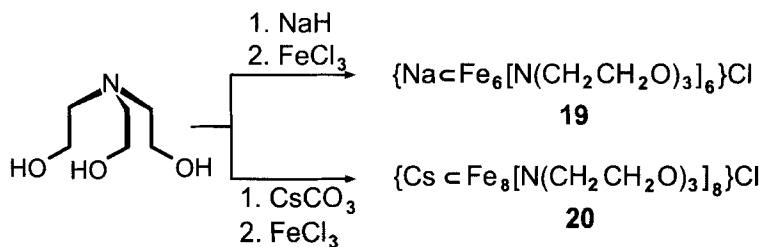


**Figure 8** X-ray crystallographic structure of cation  $[Na C Fe_6(\mu_2-OMe)_{12}(dbm)_6]^+$  of **18**.



**Scheme 2** Formation of six- and eight-membered iron coronates **19** and **20**.

structure, in which a sodium ion is encapsulated in the center, and a chloride is the counterion (Figure 9). The six crystallographically equivalent iron atoms of the centrosymmetric cation  $\{\text{Na} \subset \text{Fe}_6[\text{N}(\text{CH}_2\text{CH}_2\text{O})_3]_6\}^+$  of **19** are located in the corners of a regular hexagon. The diameter of the hexagon, defined as the distance of two opposite iron atoms, is 6.431 Å. The distorted octahedral coordination sphere of the iron atoms is composed of one nitrogen donor, one  $\mu_1$ - and two  $\mu_2$ - and two  $\mu_3$ -oxygen donors. Consequently, triethanolamine acts as a tetradentate ligand and links three iron(III) ions.

Three sets of six oxygen atoms are located in the corners of three pairs of regular triangles, which are rotated 60° relative to each other (Figure 10, left). The trigonal faces are located parallel and equidistant in pairs with one plane above and one

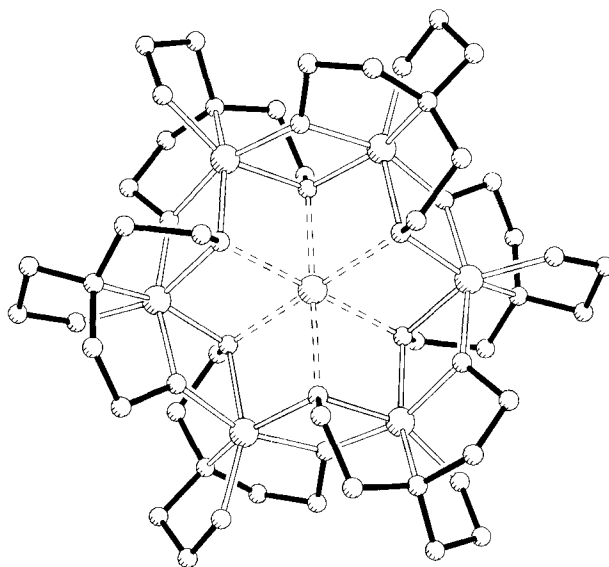


**Figure 9** X-ray crystallographic structure of cation  $\{\text{Na} \subset \text{Fe}_6[\text{N}(\text{CH}_2\text{CH}_2\text{O})_3]_6\}^+$  of **19**.

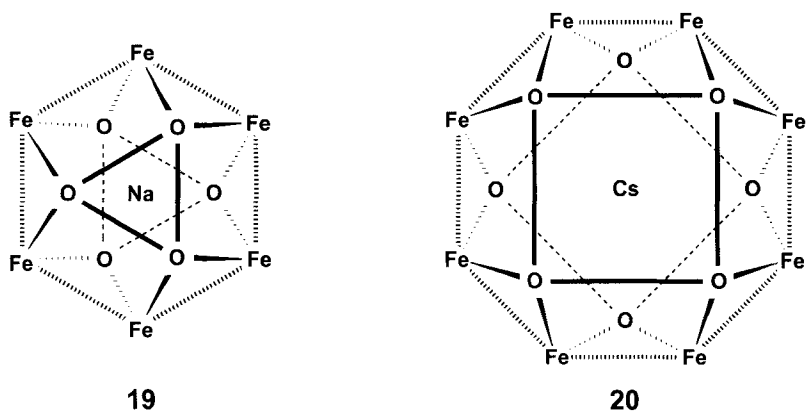


**Figure 10** Left: schematic representation of the central  $\text{Fe}_6\text{O}_6$  backbone with one set of six oxygens of **19**. Right: schematic representation of the central  $\text{Fe}_8\text{O}_8$  backbone with one set of eight oxygens of **20**.

below the hexagonal plane generated by the iron atoms. These six oxygen atoms are related by an  $S_6$  axis. The sodium ion is located in the center of the cation of **19** and has a distorted octahedral coordination sphere from the six  $\mu_3$ -O atoms. The diameter (1.98 Å) of the cavity marked by opposite  $\mu_3$ -O atoms nearly corresponds to double the ionic radius of sodium (2.04 Å).

According to Lehn *et al.* [34], in the case of the template mediated self-construction of a supramolecular system, amidst a set of possibilities, a combination of building blocks is realized, which leads to the best receptor for the substrate. Therefore, it is possible that the six-membered cyclic structure  $\{\text{Na} \subset \text{Fe}_6[\text{N}(\text{CH}_2\text{CH}_2\text{O})_3]_6\}\text{Cl}$  **19** is exclusively selected from all the imaginable iron triethanolamine oligomers, when sodium ions are present. Thus, in the presence of cations with ionic radii that differ from that of sodium, variant structures are expected.

When triethanolamine was allowed to react with cesium carbonate and iron(III) chloride (Scheme 2), an X-ray structure analysis of the reaction product **20** revealed a cyclic iron(III) complex with a [16]metallacrown-8 structure, in which the cesium was located in the center of the ring and a chloride ion functioned as counterion (Figure 11; 3D-3) [46]. The eight iron atoms of the almost centrosymmetric cation  $\{\text{Cs} \subset \text{Fe}_8[\text{N}(\text{CH}_2\text{CH}_2\text{O})_3]_8\}^+$  of **20** are located in the corners of a nearly regular octagon. The diameter of the octagon, defined as the mean distance between opposite iron atoms, is 8.224 Å. The distorted octahedral coordination sphere of the iron atoms is composed of one nitrogen donor, one  $\mu_1$ -, two  $\mu_2$ - and two  $\mu_3$ -oxygen donors.

Three sets of eight out of a total of 24 oxygen atoms are located on the corners of three pairs of square faces that are rotated  $45^\circ$  relative to each other (Figure 10,

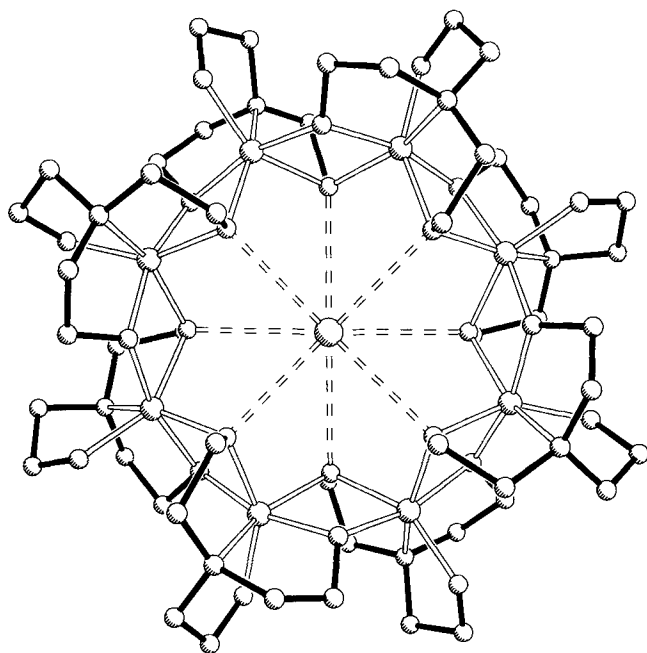


**Figure 11** X-ray crystallographic structure of cation  $\{\text{Cs} \subset \text{Fe}_8[\text{N}(\text{CH}_2\text{CH}_2\text{O})_3]_8\}^+$  of **20**.

right). The square faces are located parallel and almost equidistant in pairs and one plane lies above and one below the octagon generated by the iron atoms. These structural elements share a common  $S_8$  axis. The cesium ion lies directly above the center of the cation of **20** and is shifted about 0.5 Å towards the chloride counterion. The eight  $\mu_3$ -O atoms form a quadratic antiprism coordination sphere around the cesium center. Furthermore, a common feature of complexes **19** and **20** is that the  $\mu_1$ -O atoms do not participate in the formation of the hexa- and octanuclear structures. They solely function as ligands and for the coordinative saturation of the iron atoms. However, other donors such as chloride ions could also be candidates for this function. Therefore, *N*-methyl-diethanolamine was allowed to react with calcium hydride and iron(III) chloride. According to the X-ray crystallographic analysis, product **21** is present in the crystal as an unoccupied neutral iron(III) complex with a [12]metallacrown-6-structure (Figure 12).

The six iron atoms of the approximately centrosymmetric neutral molecule  $\{\text{Fe}_6[\text{H}_3\text{C}-\text{N}(\text{CH}_2\text{CH}_2\text{O})_2]_6\text{Cl}_6\}$  **21** are located in the corners of an almost regular hexagon. The diameter of the hexagon, defined as the mean distance between two opposite iron atoms, is 6.361 Å. The distorted octahedral coordination sphere of the iron atoms is composed of one nitrogen donor, one chloride ion, and four  $\mu_2$ -oxygen donors.



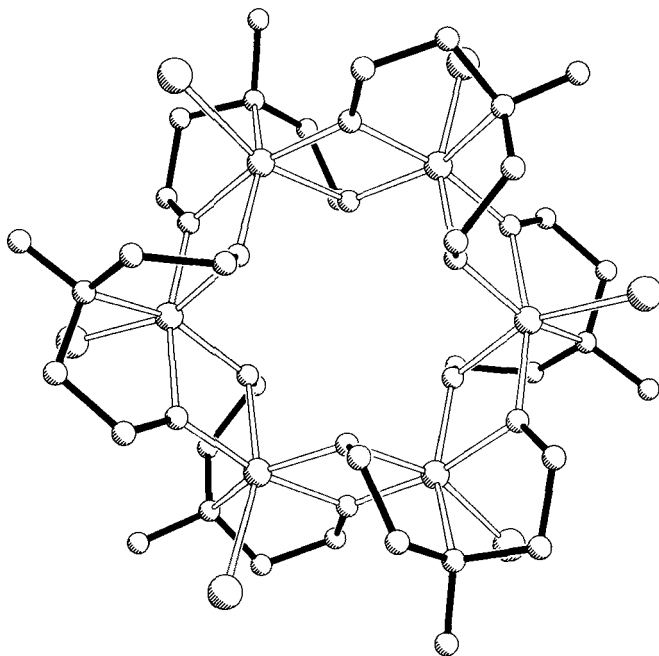


**Figure 12** X-ray crystallographic structure of  $\{\text{Fe}_6[\text{H}_3\text{C}-\text{N}(\text{CH}_2\text{CH}_2\text{O})_2]_6\text{Cl}_6\}$  **21**.

Most of the oligonuclear cyclic chelate complexes were discovered by serendipity. This is also true for  $\{\text{Zn} \subset [\text{Zn}(\text{hmp})_2]_6\}\text{Cl}_2$  **22** which was generated from  $\text{Zn}[\text{N}(\text{SiMe}_3)_2]_2$  and 2-hydroxymethylpyridine (Hhmp) in the presence of  $\text{CHCl}_3$  or  $\text{CH}_2\text{Cl}_2$  [56]. The pictogram of **22** (Figure 13) indicates the high symmetry of the complex dication composed of a central  $\text{Zn}^{2+}$  ion surrounded in a disk-like fashion by six  $\text{ZnO}_2\text{N}_2$  fragments.

Interestingly, the reaction between  $\text{MnCl}_2 \cdot 4\text{H}_2\text{O}$ , 2-hydroxymethylpyridine (Hhmp) and  $\text{NEt}_4\text{MnO}_4$  in acetonitrile gives the mixed-valence manganese cluster topology  $\{\text{Mn} \subset [\text{Mn}_6(\text{OH})_3\text{Cl}_3(\text{hmp})_9]\}\text{Cl}[\text{MnCl}_4]$  **23**, in which three  $\text{Mn}^{\text{II}}$  and three  $\text{Mn}^{\text{III}}$  cations comprise a  $\text{Mn}_6$  hexagon [57]. The central  $\text{Mn}^{\text{II}}$  ion is held by three  $\mu_3\text{-OH}^-$  and three  $\mu_3\text{-O}_{\text{hmp}}^-$  ions, the latter bridging two peripheral and the central manganese atoms. The remaining  $\mu_2\text{-O}_{\text{hmp}}^-$  ions bridge the manganese atoms of the hexagon. The complexed dication of **23** has virtual  $\text{C}_3$  symmetry. The  $\text{Cl}^-$  counterion is hydrogen bonded to the  $\mu_3\text{-OH}^-$  groups, but the  $\text{NEt}_4^+$  and  $\text{MnCl}_4^{2-}$  ions are well separated from the nearly planar  $\text{Mn}_7$  unit (Figure 14).

In some cases the conditions are even more complex. For instance, it has been shown, that two metallacoronates, containing 17 and 19 iron(III) ions, respectively, crystallize together in the same unit cell and have very similar structures and formulas [53,58]. That of trication  $\{\text{Fe} \subset [\text{Fe}_{16}(\mu_3\text{-O})_4(\mu_3\text{-OH})_6$

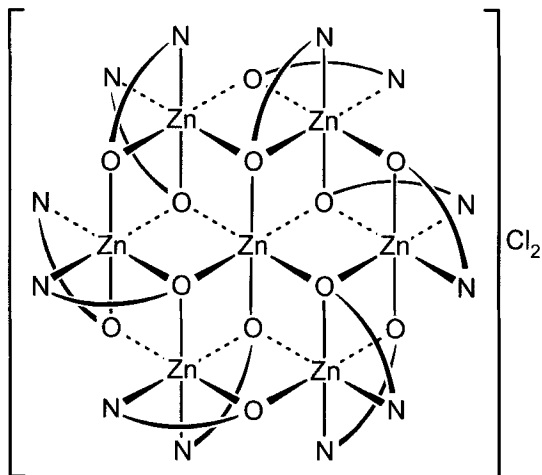


**Figure 13** Pictorial representation of  $\{Zn \subset [Zn(hmp)_2]_6\}Cl_2$  **22**.

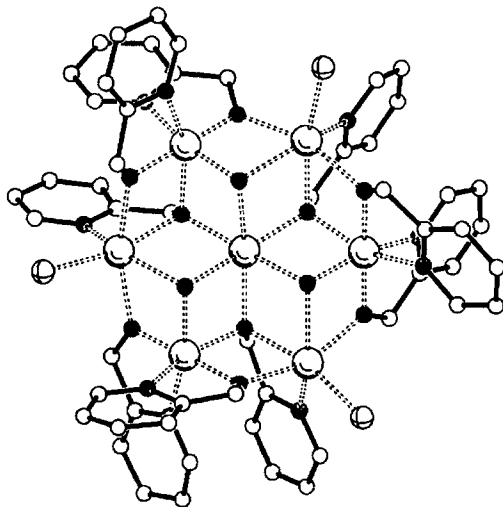


**Figure 14** X-ray crystallographic structure of cation  $\{Mn \subset [Mn_6(OH)_3Cl_3(hmp)_9]\}^{2+}$  of **23**.

$(\mu_2-OH)_{10}(heidi)_8(H_2O)_{12}\}^{3+}$  **24** [ $H_3heidi = HO(CH_2)_2N(CH_2CO_2H)_2$ ] is shown in Figure 15. It is interesting to note that the central core of **24**, which is composed of seven iron ions is very similar to that observed for the cation  $[Na \subset Fe_6(\mu_2-OMe)_{12}(dbm)_6]^+$  of **18** [53].

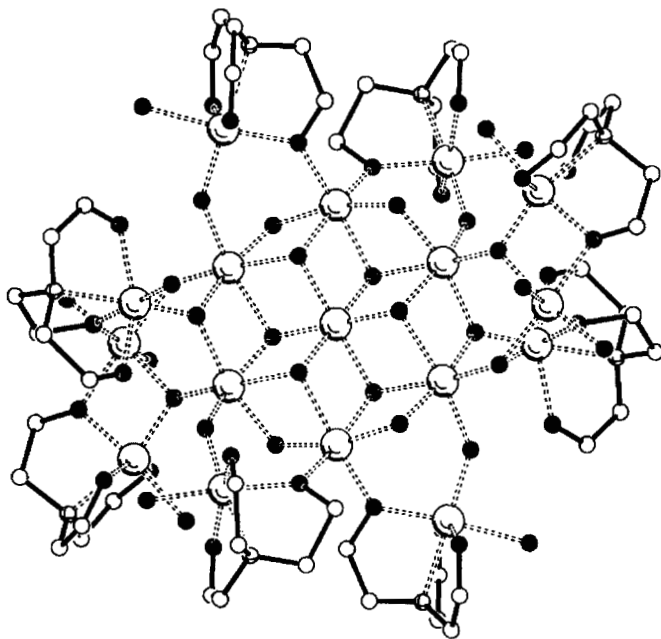


**Figure 15** X-ray crystallographic structure of trication  $[\text{Fe} \subset [\text{Fe}_{16}(\mu_3\text{-OH})_4(\mu_3\text{-OH})_6(\mu_2\text{-OH})_{10}(\text{heidi})_8(\text{H}_2\text{O})_{12}]]^{3+}$  of **24**.

The ring size does not necessarily determine the diameter of the hole of a metallocoronate, as was shown by the cyclic structure  $[\text{Fe}(\text{OMe})_2(\text{O}_2\text{CCH}_2\text{Cl})]_{10}$  **25** (Figure 16), better known as *ferric wheel* [11,48,53]. The *wheel* is prepared in methanol solution from the reaction between  $[\text{Fe}_3\text{O}(\text{O}_2\text{CCH}_2\text{Cl})_6(\text{H}_2\text{O})_3](\text{NO}_3)$  and  $\text{Fe}(\text{NO}_3)_3 \cdot 9\text{H}_2\text{O}$ . Four  $\mu_2$ -OMe donors and two monochloroacetate ions link three Fe(III) ions each out of the 10 Fe(III) ions of **25** and is unoccupied in the center.

Similarly, toroidal inclusion complex  $\{(\text{NH}_4) \subset [\text{Co}(\text{OMe})_2(\text{O}_2\text{CMe})]_8[\text{PF}_6]\}$  is isolated from the reaction between cobalt(III) acetate and methanol in the presence of  $\text{NH}_4\text{PF}_6$  [59].

Recently a hexadecanuclear polyolatometalate of copper(II) and multideprotonated D-sorbitol was synthesized and characterized by X-ray diffraction [60]. However, the hitherto largest cyclic  $\text{Fe}^{\text{III}}$  cluster contains 18 iron(III) ions in the ring. The octadecairon(III) complex  $[\text{Fe}(\text{OH})(\text{XDK})\text{Fe}_2\text{OMe})_4(\text{O}_2\text{CMe})_2]_6$  **26** [where  $\text{H}_2\text{XDK} = m$ -xylilene diamine bis(Kemp's triacid imide)] [61] was prepared in the presence of tetraalkylammonium carboxylate salts from slightly alkaline methanolic solutions of the diiron(III) complex  $[\text{Fe}_2\text{O}(\text{XDK})(\text{HOMe})_5(\text{H}_2\text{O})](\text{NO}_3)_2 \cdot 4\text{H}_2\text{O}$ . The composition of the crystalline product, a double salt having the formula **26**·6 $\text{Et}_4\text{N}(\text{NO}_3)$ ·15 $\text{HOMe}$ ·6 $\text{Et}_2\text{O}$ ·24 $\text{H}_2\text{O}$ , was determined by microanalysis and a single-crystal X-ray diffraction analysis (Figure 17). The

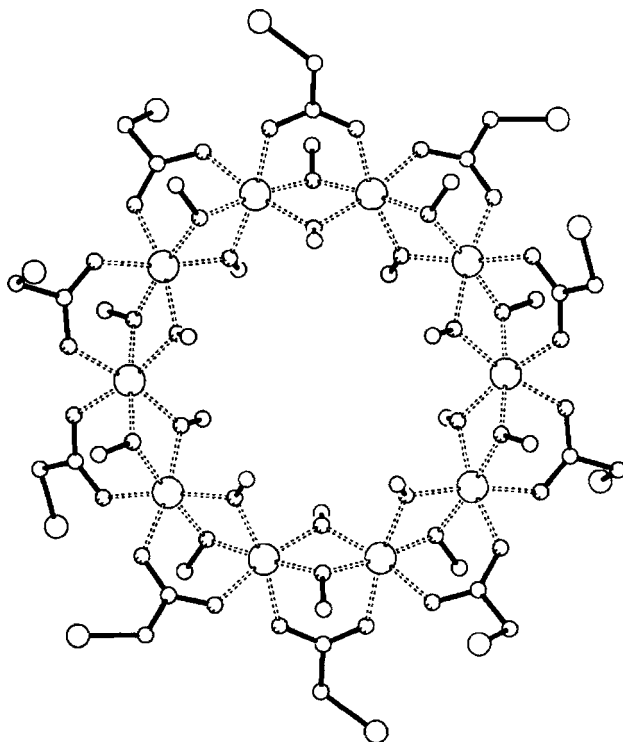


**Figure 16** X-ray crystallographic structure of  $[\text{Fe}(\text{OMe})_2(\text{O}_2\text{CCH}_2\text{Cl})]_{10}$  **25**.

molecular 18-wheeler has idealized  $D_{3d}$  symmetry. The repeating unit comprises a ( $\mu$ -hydroxo)bis( $\mu$ -carboxylato)-diiron(III) moiety linked by an acetate and two methoxide ions to a third iron atom. Each iron atom in **26** has distorted octahedral symmetry. The hydrophobic environment afforded by the  $\text{XDK}^{2-}$  ligands on the inner surface of the wheel is incompatible with its occupancy by cations, as seen in the case of smaller metallocoronates lacking this feature [2,19,43–47,51–53].

The study of molecules possessing unusual large spin values in their ground state is an area of current interest [50,57,61,62]. It has recently become apparent that a relatively high ground-state spin value is one of the necessary requirements for molecules exhibiting single-molecule magnetism. The synthesis of new high-spin molecules is thus of interest.

Oxalate (ox) is widely used to prepare molecular-based magnetic materials. The structures of  $(\text{NBu}_4)[\text{Mn}^{\text{II}}\text{Cr}^{\text{III}}(\text{ox})_3]$  and  $(\text{PPh}_4)[\text{Mn}^{\text{II}}\text{Cr}^{\text{III}}(\text{ox})_3]$  have been determined and shown to be lamellar and isostructural. In the layer planes, each  $\text{Mn}^{\text{II}}$  ion is bound to three  $\text{Cr}^{\text{III}}$  ions (and vice versa) via oxalato bridges generating a graphite-like pattern. The repeating unit  $[\text{Mn}^{\text{II}}\text{Cr}^{\text{III}}(\text{ox})_3]^-$  **27** is reminiscent of a heteronuclear metallocrown ether and is represented schematically in Figure 18 [63].

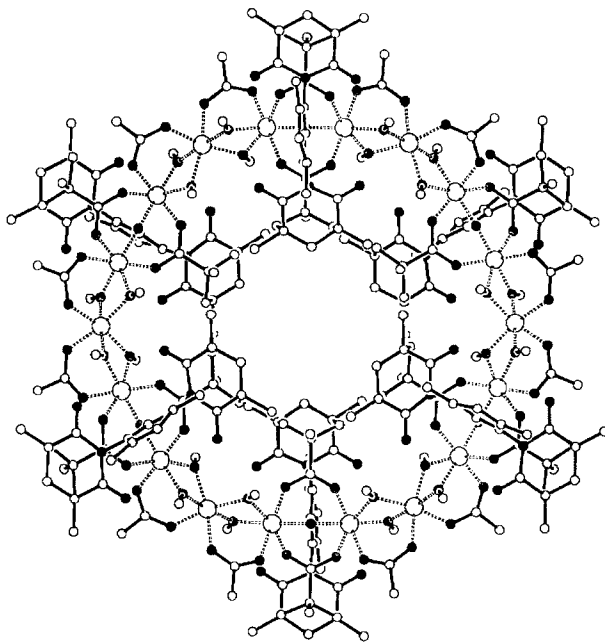


**Figure 17** X-ray crystallographic structure of  $[\text{Fe}(\text{OH})(\text{XDK})\text{Fe}_2(\text{OMe})_4(\text{O}_2\text{CMe})_2]_6$  **26**.

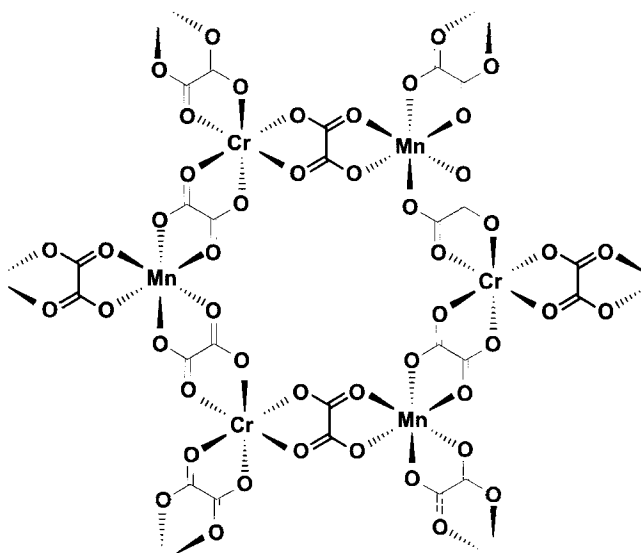


**Figure 18** Schematic representation of the repeat unit **27** of  ${}^2_{\infty}[\text{Mn}^{\text{II}}\text{Cr}^{\text{III}}(\text{ox})_3]^-$  without the bulky cations being located between adjacent layers.

## 2.2 Circular Helicates

Inorganic double or triple helices are formed by two or three ligand strands wrapped around linearly disposed metal ions [13]. Among cyclic transition metal complexes, circular helicates  $[n]^m\text{cH}$  ( $[n]^m\text{cH}$  is a general notation characterizing circular helicates ( $\text{cH}$ ) with  $n$  = number of metal ions and  $m$  = helicity ( $m=2$  for a double helix)) have specific features and may be considered as toroidal helices [34]. There are two different kinds of circular helical systems. Some structures self-assemble from the metal ions and the ligands only in the presence of an anion, which could act as a template [34,35,64–67], whereas, in other cases, the circular helicates self-assemble from the metal ions and the ligands alone [68–70].

### 2.2.1 Anion-centered circular helicates

The interest in polynuclear supramolecular iron complexes mainly stems from the importance of oxo-centered polyiron aggregates as model compounds for iron-oxo proteins. In principle,  $\mu_3$ -oxo-centered complexes related to  $[\text{Fe}_3\text{O}(\text{O}_2\text{CR})_6(\text{H}_2\text{O})_3]$  **28** [71] (Figure 19, left) should also be accessible with other double negatively charged ligands. Double deprotonation of  $\text{H}_2\text{L}$  **29** gives rise to two dianionic rotamers ( $\text{L}^{\text{A}}\text{}^{2-}$  and  $\text{L}^{\text{B}}\text{}^{2-}$ , which with  $\text{Fe}^{\text{III}}$  or  $\text{Zn}^{\text{II}}$  ions selectively furnish two different complexes  $[\text{Fe}_3\text{OL}^{\text{A}}_3]$  **30** [35] and  $[\text{Zn}_8\text{O}_2\text{L}^{\text{B}}_6]$  **31** (Scheme 3) [64].

According to the X-ray crystallographic analysis, **30** is present in the crystal as a neutral, trinuclear, iron chelate complex (Figure 19, right; 3D-4). The core of

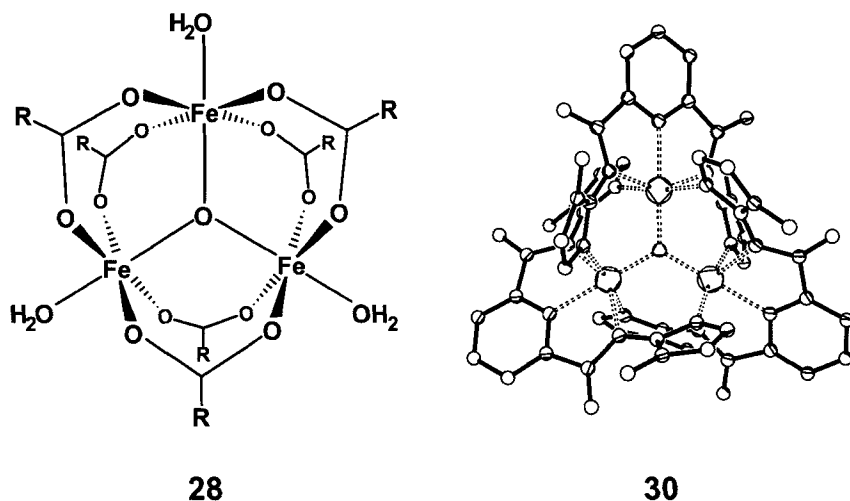


**Figure 19** Left: schematic representation of  $[\text{Fe}_3\text{O}(\text{O}_2\text{CR})_6(\text{H}_2\text{O})_3]$  **28**. Right: X-ray crystallographic structure of  $[\text{Fe}_3\text{OL}^{\text{A}}_3]$  **30**.